Article

Not peer-reviewed version

A Procedure for Analyzing Vertical Ground Deformation Anomalies in Active Volcanic Caldera during Unrest Phases

Fabio Matano *, Annarita Casaburi, Giuseppe De Natale

Posted Date: 11 September 2024

doi: 10.20944/preprints202409.0809.v1

Keywords: caldera unrest; ground deformation; volcanic hazard; MT-InSAR; Sentinel-1

Article

A Procedure for Analyzing Vertical Ground Deformation Anomalies in Active Volcanic Caldera during Unrest Phases

Fabio Matano [1,*], Annarita Casaburi [1] and Giuseppe De Natale [2]

[1] CNR-ISMAR - Consiglio Nazionale delle Ricerche, Istituto di Scienze Marine, Napoli, Italy
[2] INGV - Istituto Nazionale di Geofisica e Vulcanologia, Osservatorio Vesuviano, Napoli, Italy
* Correspondence: fabio.matano@cnr.it

Abstract: Collapse calderas often experience large up and down movements, which rarely give rise to eruptions. The pattern of vertical deformation has generally an elliptical geometry, very close to a circular one. A simple and powerful method to explore second order anomalies of the volcanic caldera deformation patterns can enlighten important structural features. This method is here presented and applied to the case study of Campi Flegrei caldera ground deformation, representing a typical example of such a quasi-circular geometry, with dominant ground uplift occurring since 1950. Despite a markedly radial dependence of the vertical displacement, with a very constant shape in the time, we explore in the paper the second order anomalies, with respect to a purely radial behavior. To this aim, we have used a procedure based on the polynomial fit of the vertical displacement data, assuming they only depend on the distance from the maximum uplift point (i.e. deformation center); then, we have obtained anomalies map by subtracting from the theoretical deformation so determined the true data. We then obtain very peculiar results, which put in evidence a sharp separation between a less uplifted zone and a more uplifted one than expected, along a NE-SW alignment which approximately define the most seismically active area, in which most of the largest magnitude earthquakes occur. This very peculiar feature is likely to represent a main volcano-tectonic structure in the area, which can be of leading importance for evaluating both the highest seismic hazard area and the most likely zone of possible eruptive vent opening. The results obtained here indicate that the proposed method can be useful to analyze unrest related hazards.

Keywords: caldera unrest; ground deformation; volcanic hazard; MT-InSAR; Sentinel-1

1. Introduction

Calderas are subcircular depressions that form during the partial emptying of magma reservoirs associated with large eruptions. A number of calderas are marked by the uplift (resurgence) of their sunken floor, resulting from magma accumulation and accompanied by minor eruptions. This inversion of the negative topography of a caldera represents the largest and most protracted type of volcanic ground deformation, with amounts ranging from a few hundred to a thousand meters and a duration up to several thousand years [1]. The processes that regulate caldera uplift generally relate resurgence to the input of new magma, which is often stimulated by the pressure drop that follows a caldera forming eruption [2–4]. However, part of the caldera resurgence can be related to the increase of pressure of the geothermal system, as a consequence of the heating due to magmatic gas inflow [5–7].

Unrest episodes may be indicative of short-term inflation events that give rise to caldera resurgence [8]. The majority of volcanic eruptions are preceded and accompanied by a period of unrest, defined as a change from the normal state or baseline behavior of a volcano. Large calderas

 doi:10.20944/preprints202409.0809.v1

may show episodes of unrest that commonly occur for years, decades or centuries, with or without a following eruption [9–11].

The potential hazards associated with unrest include also volcano-tectonic seismicity, ground uplift and surface deformation, hydrothermal explosions or gas emissions, faults and fractures opening, increased degassing, and landslides [9,12]. Such events may result in significant physical damage to buildings, critical infrastructures (i.e. electricity, telecommunications, water and sewerage networks), roads and railways, harbor functionality [13,14]. These damages may also result in significant economic loss through business interruption, tourism income drop, decreases in property values and increases in insurance premiums [12,14–16].

Ground deformation during unrest phases is characterized by high uplift and/or subsidence rates, related to inflation and deflation of the caldera floor due to magmatic and/or hydrothermal processes usually characterized by a marked radial or elliptical symmetry (first order ground deformation) rapidly decreasing with distance from the caldera center.

Investigations of spatial variability of the unrest-related ground deformation have been rarely made and often the local (or second order) ground deformation anomalies, related to the activity of volcano-tectonic faults, secondary inflation centers or other, are underestimated or ignored. This leads to deficiencies in hazard analysis due to phenomena related to unrest phases and may hidden the identification of possible pathways for magma rising, eventually leading to an eruption.

In this paper we propose a simple procedure for filtering first order ground deformation radial signal in active volcanic caldera during unrest phases by using Sentinel-1 Synthetic Aperture Radar Multi-Temporal Interferometry (MT-InSAR) data, in order to highlight second order ground deformations or anomalies that characterize the complex volcano-tectonic evolution of a caldera unrest.

The proposed procedure has been applied to the Campi Flegrei caldera case study, that is currently ongoing an unrest phase characterized by un uplift of 139 cm since November 2005 to June 2024 at the RITE GNNS station located at the Pozzuoli historical center, with average velocity rates of 20 +/- 3 mm/month since April 2024 [17]. Seismic activity has increased progressively during the unrest, both in frequency and in maximum magnitude [7], to reach a magnitude Md=4.4, for a seismic event occurred on 2024/05/20 [17]. The Campi Flegrei caldera already experienced significant seismicity associated to volcanic unrest between 1970-72 and 1982-84 [7,13], but hazard assessments in this region have concentrated on eruption hazards, rather than on those resulting from volcanic unrest [12]. We are going to show, in this paper, that the analysis of second order ground deformations (or anomalies) can help in the hazard analysis related to volcano-tectonic seismicity, as well as to detect main faults, fractures, structural features and most likely areas of possible vent opening.

2. Study Area

The 12-km sized active Campi Flegrei caldera (Figure 1) is located in southern Italy, westward Naples town, and is characterized by a volcanic activity started between the late Middle and the early Upper Pleistocene prior to 80 ka BP [18,19]. Until few years ago, Campi Flegrei was considered a nested caldera [e.g. 20,21], generated by two collapses occurred 40 ka BP (Campanian Ignimbrite: [22,23]) and 15 ka BP (Neapolitan Yellow Tuff eruption: [20,24–26]. However, De Natale et al. [27,28] and Rolandi et al. [29] have recently demonstrated that Campanian Ignimbrite occurred North of the Campi Flegrei caldera and did not cause any collapse. Campi Flegrei caldera has been then generated by the Neapolitan Yellow Tuff (NYT) eruption (15 ka). The post-15 ka evolution of the NYT caldera was marked by the development of a resurgent dome in the inner part of the caldera (Figure 1), including the proximal sector of the Pozzuoli Bay, characterized by an uplift of about 100 m [11,30,31]. The dome resurgence resulted in the emersion of marine deposits forming the so-called La Starza terrace (Figure 1), which is presently exposed up to ~30 m above sea level [32].

The post-collapse volcanic activity was characterized by over 70 events (Figure 1) post-15 ka concentrated in three main epochs separated by two quiescent periods [33–36]. The first epoch (15 to ~9.5 ka BP) is characterized by several explosive events, of which Pomici Principali eruption was the

Preprints.org (www.preprints.org) | NOT PEER-REVIEWED | Posted: 11 September 2024 doi:10.20944/preprints202409.0809.v1

most energetic one [33,37]. The second epoch (8.6-8.2 ka BP [33]) is distinguished by only a few episodes of low-magnitude eruptions. The third epoch activity began between 4.4 and 3.8 ka BP and was characterized by several explosive events [33] of which the Agnano-Monte Spina eruption (4.4 ka BP [38,39]) was the most powerful one; not only of the third epoch, but among all the post-caldera eruptions. This epoch was followed by a prolonged period of volcanic quiescence that persists until today, interrupted only by the Monte Nuovo eruption in 1538 AD, a small phreato-magmatic one with VEI=2 [40–44].

The geology of the study area is mainly characterized by volcanic units, made by pyroclastic deposits, tuffs and ignimbrites, and by recent alluvial, colluvial, slope and coastal deposits (Figure 1). The main volcano tectonic structure is formed by the structural rims forming the NYT caldera [32,45–47], as clearly recognized in the Pozzuoli Bay offshore by the presence of a ring-fault system [31,32,48,49]. N–S trending fault segments, including the Bacoli and Baia faults and the Monte Nuovo fault, delimit the western inner border of the caldera; several E-W, NW-SE and NE-SW trending fault segments are present within the central resurgent area and the eastern caldera border (Figure 1). The observed crosscutting relationships indicate that the recent E-W and N-S structures overprint the NE-SW and NW-SE lineaments, that are inherited regional trends linked to the Pleistocene extensional tectonics [30,46,50,51].

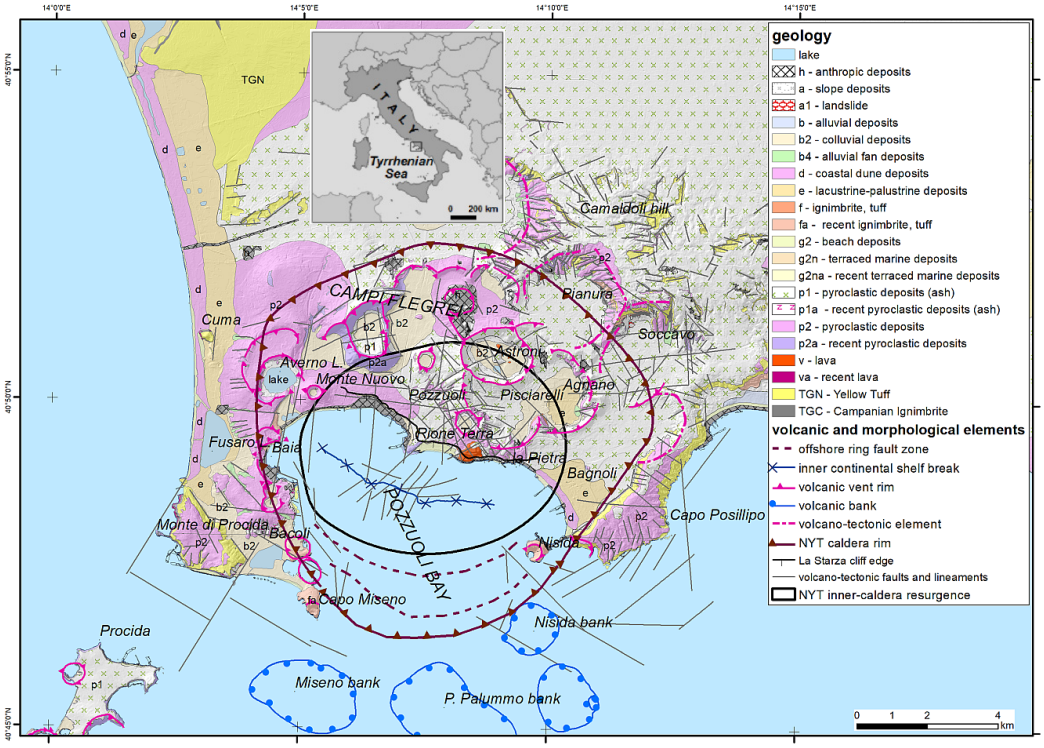

Figure 1. Geological map of the Campi Flegrei caldera. Volcanic and morphological elements by Sacchi et al. [32] and reference therein; volcano-tectonic faults and lineaments by Natale et al. [47].

2.1. Ground Deformation in Historical Times

During the last 2100 years, the central sector of the Campi Flegrei caldera has undergone alternating phases of subsidence and uplift in the range of about 20 meters with maximum values centered in the Pozzuoli city area, associated with fumarolic and hydrothermal processes, that is locally referred to as bradyseism (e.g. [52,53]).

A long subsidence phase (about 18 m) continued at least since the Republic Roman Age (II-III centuries b.C.) to the Middle Age around the XV century, probably interrupted by an uplift during the V-VIII century. A strong uplift (about 16 m) occurred for almost a century before the Monte Nuovo eruption (1538 AD) [44,54,55].

 doi:10.20944/preprints202409.0809.v1

The quiescence after the 1538 eruption has been characterized by a progressive subsidence more than 8 m in the central sector) of the caldera area, lasted until 1950. Since such date, a new period of intermittent uplift has begun, with the unrest episodes occurred in 1950-1951, 1969-1972, 1982-1984, during which the ground uplift at the port of Pozzuoli town reached about 4 m with respect to the ground level before 1950 (Figure 2). After the end of 1984, the ground subsided of about 0.94 m, until the end of 2005. Since the last months of 2005, ground uplift started again, and is still in progress (Figure 2); total uplift for the ongoing unrest has reached 1.39 m at the end of June 2024 [17].

The origin of this inflation-deflation deformation is still under debate and may be related to the magma intrusion, pressurization-depressurization of the hydrothermal system, or both [45,56–62].

The ground uplift of the 1950-1951 was not accompanied by felt seismicity and during the 1969-1972 seismicity was of very low magnitude, up to about M=2.1. During the period 1983-1984, on the contrary, seismicity was very frequent (about 16.000 earthquakes recorded by the analogue seismic network of the time) and with significant magnitude (Mmax=4.0) [30,63,64] and a total ground uplift of 1.8 m was recorded (Figure 3) near the town center of Pozzuoli [65]. Seismic activity was characterized by Md=4.0 in 1983.10.04 and Md=3.8 in 1984.12.08 events, resulting in substantial damage to buildings and the evacuation of over 40,000 residents from the central town of Pozzuoli. Seismicity here is very shallow (in the first 3 km of the crust) so that even earthquakes of magnitude 4 or lower can be very damaging for the closest buildings, in this very densely urbanized area.

Then, a subsidence of about 1 m during 1985-2005 occurred. In the last two decades, the central portion of Campi Flegrei caldera has experienced ground uplift of about 1.4 m, and an increase in magnitude and extent of seismicity, especially since 2021 [17,66].

During the ongoing unrest, although the uplift rate is much lower than in the ‘70s and ‘80s, seismicity has reached maximum magnitude higher than ever, with an earthquake of M=4.2 occurred on September 27th, 2023, and the strongest one of M=4.4 occurred on May 20th, 2024. The progressive increase of earthquake frequency and maximum magnitude had been already clearly forecasted [7,67], as due to the progressive increase of underground pressure, which also generate the progressive increase of ground level. Some recent papers (i.e. [68]) have identified some of the main faults and volcano-tectonic structures of the area, from precise earthquake locations; but, as we will show in this paper, static displacement anomalies from MT-InSAR data analyses can be even more powerful indicators of structural features.

The pattern of ground deformation during the recent bradyseismic episodes displays maximum values at Pozzuoli harbor and is characterized by a rapid radial decay of the deformation that becomes minimal at a distance of 6 km from the center [69–71]. The decay seems homogenous at large scale and its geometry does not change over time.

Preprints.org (www.preprints.org) | NOT PEER-REVIEWED | Posted: 11 September 2024 doi:10.20944/preprints202409.0809.v1

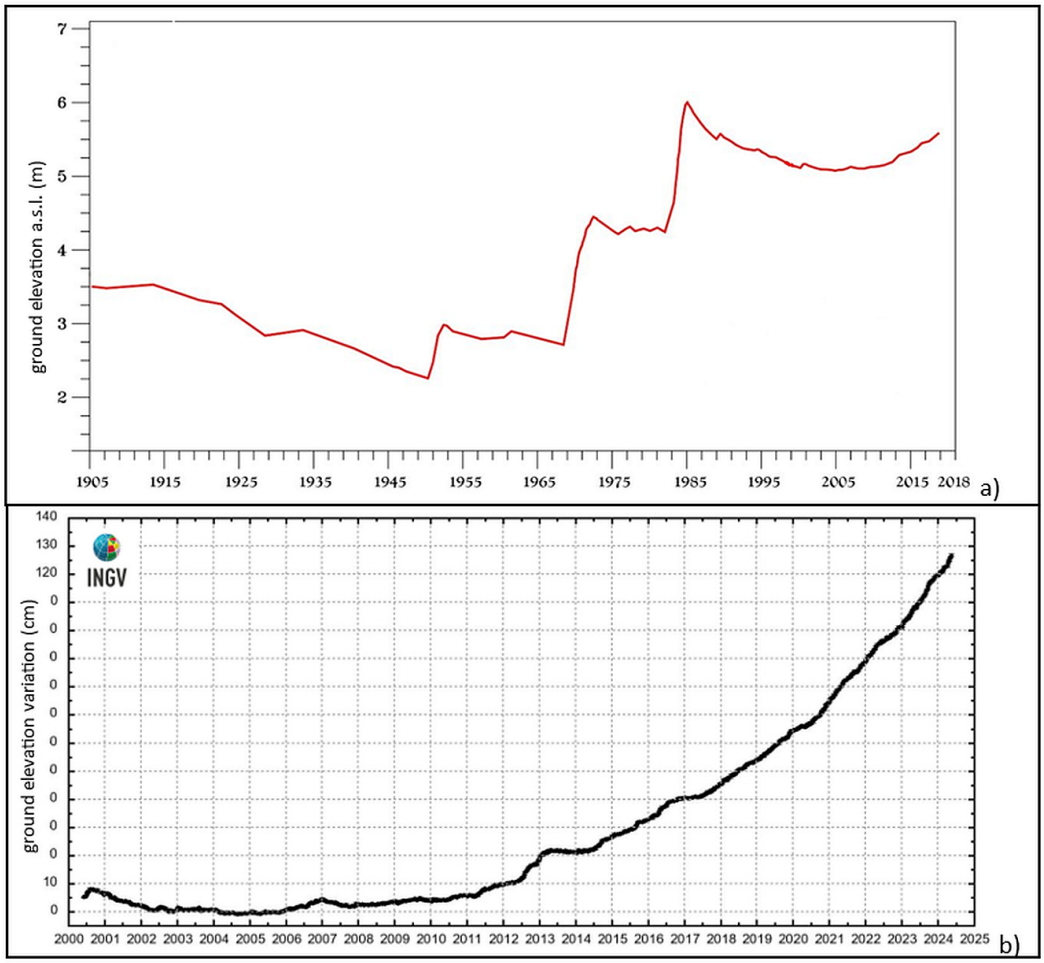

Figure 2. Ground deformation trend, located in the maximum deformation area close to "Rione Terra" district in the Pozzuoli city center: a) levelling measurements from 1905 to 2017 at the altimetric benchmark 25A [64,72]; b) GNNS measurements at the RITE station from June 2000 to June 2024 [17].

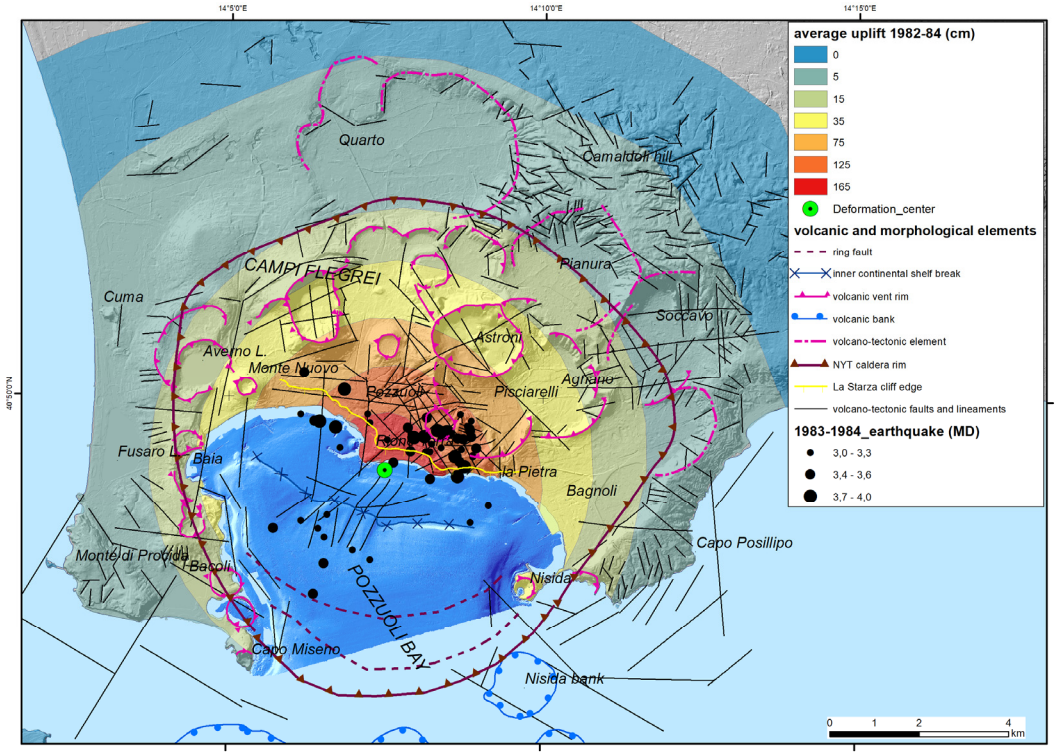

 doi:10.20944/preprints202409.0809.v1

Figure 3. Ground deformation cumulative uplift during the 1982-84 bradyseismic crisis [73,74]. 1983-84 earthquake epicenters by INGV-GOSSIP; DEM of sea floor in the Pozzuoli Bay by Somma et al. [75].

3. Methods

Monitoring of ground deformation at Campi Flegrei has been carried out through ground-based topographic leveling networks since 1905 [64]. Since the 2000's years this classic geodetic system has been integrated with a permanent Global Positioning System (GPS) monitoring network on land [76,77].

In the last decade MT-InSAR has become a powerful technique for measuring slow ground-surface deformation movements occurring in a range of dynamic processes, including volcanism and volcano-tectonics processes [78–80]. MT-InSAR technique provides very accurate, unidimensional, millimetric measurements of ground movements along the Line-Of-Sight (LOS), the straight line between radar sensor and the target [81,82]. Differential inteferometric SAR techniques have given an overall perspective on the spatial distribution of recent ground deformation in Campi Flegrei area, exploiting the C-band sensors onboard ERS (from 1992 to 2001), ENVISAT (from 2002 to 2010) and RADARSAT (from 2003 to 2007) satellites in several papers [71,80,83,84].

In this paper Ground Deformation Movements (VGDM) were assessed for the Jan. 2016 – Dec. 2021 interval by analyzing European Ground Motion Service (EGMS) data in vertical and horizontal polarizations. EGMS is implemented by the European Space Agency processing Synthetic Aperture Radar (SAR) images of Sentinel-1 satellites constellation [85,86] to provide Advanced Differential Interferometric SAR (A-DInSAR) data over the main part of Europe territory since 2015 (https://land.copernicus.eu/en/products/european-ground-motion-service). This service processes average velocities and deformation time series, derived by both Persistent Scatterers [87] and Distributed Scatterers [88,89] technics. EGMS provides data at full resolution (20 by 5 m) in the satellite LOS locally referenced (basic product) or GNNS globally referenced (calibrated product), and finally two Orho datasets by combining DInSAR displacement calibrated data of ascending and descending orbits resampled to a 100 m grid. One of the layers is a purely vertical displacement (EGMS Ortho Vertical), while the other is a purely east-west horizontal displacement (EGMS Ortho East/West) in a final resolution of 100 by 100 m. All these datasets were downloaded and imported in a Geographic Information System (GIS) to identify the places with active ground deformation process in the Campi Flegrei area.

The Ortho Vertical dataset was implemented by calculating for each point the distance to the caldera maximum deformation center, as defined by several authors [56,77,90,91].

The analysis and computation procedures involved the use of both ArcGIS and R softwares. Initially, the distance to the deformation center (denoted as r) was calculated using ArcGIS. These calculated distances were then imported into R, along with the vertical uplift values (z) that were measured by satellites at each specific point. Then, a series of polynomial curves describing the theoretical radial ground deformation with a progressively higher accuracy were generated by using the imported r and z values for each point. These polynomials were derived up to the sixth degree, as illustrated in Figure 4. To assess the fit of these curves, the R-squared values for each polynomial were calculated (Table 1). Values of "r" lower than 500 m have not been considered for the calculation of the polynomial curves considering that many sectors within this distance to the deformation center fall in the sea and few uplift values are available.

On the basis of the R-squared values and the best-fitting of the curve with point data, the sixth-grade equation (1) was selected for further analyses. The predicted uplift values for each point were calculated based on this equation:

$$y = -5E\text{-}21x^6 + 2E\text{-}16x^5 - 3E\text{-}12x^4 + 2E\text{-}08x^3 - 6E\text{-}05x^2 - 0{,}0975x + 596{,}26 \quad (1)$$

where:
x = r (distance to the deformation center)
y = z (vertical uplift value in the EGMS Ortho Vertical dataset)

 doi:10.20944/preprints202409.0809.v1

The obtained predicted values were then imported back into GIS project for further spatial analysis. A comparison was made between the predicted uplift values and the actual satellite-measured uplift values for each point. To evaluate the accuracy of the predictions, residuals were calculated. Residuals are the differences between the expected (predicted) values and the observed (measured) values of z. These residuals were then mapped to visualize the spatial distribution of discrepancies (anomalies) between the predicted and measured uplift values.

On the resultant map, areas with very negative residuals are highlighted in red, indicating regions where the uplift is significantly higher than the predicted values. Conversely, areas shaded in blue indicate regions where the residuals are positive, signifying that the observed uplift is less than what was predicted by the polynomial models.

The spatial representation of these residuals provides valuable insights into the deformation patterns and allows for a better understanding of the areas experiencing significant differences in uplift or subsidence with reference to a simple radial circular model. By identifying these discrepancies, it is possible to refine models and improve the accuracy of future predictions.

In order to analyze possible correlation between obtained deformation residuals with seismic activity and volcano-tectonic dynamics, two earthquake and fault datasets, mapped in Figure 5, where considered.

The seismic dataset was obtained by INGV on-line databases. We have considered only seismic events with magnitude greater than 3.0 occurred since 1983 in the Campi Flegrei area and surroundings. These earthquakes were clustered during 1983-84 and 2017-2024 time periods corresponding to the most relevant bradyseismic crises.

In detail we have collected data referred to all seismic events occurred since 1985 within the study area of Campi Flegrei by INGV (Istituto Nazionale di Geofisica e Vulcanologia) national earthquake list available at the link https://terremoti.ingv.it/en. These data were implemented by the INGV regional earthquake list available at the link https://terremoti.ov.ingv.it/gossip/flegrei/years.html, specifically referred to the Campi Flegrei volcanic area for years 1983-84 and 2005-24 [92].

The datasets of volcanic (caldera boundaries, crater rims, volcanic banks) and morphological elements are derived by Sacchi et al. [31,32] and Steinmann et al. [48,49], volcano-tectonic faults and lineaments by Natale et al. [93,94], while the offshore faults by Natale et al. [47,95].

Table 1. R-squared values for calculated polynomial curve.

Polynomial degree	R-squared value
sixth	**0.9891**
fifth	0.9879
fourth	0.9871
third	0.9831
second	0.8999

Preprints.org (www.preprints.org) | NOT PEER-REVIEWED | Posted: 11 September 2024 doi:10.20944/preprints202409.0809.v1

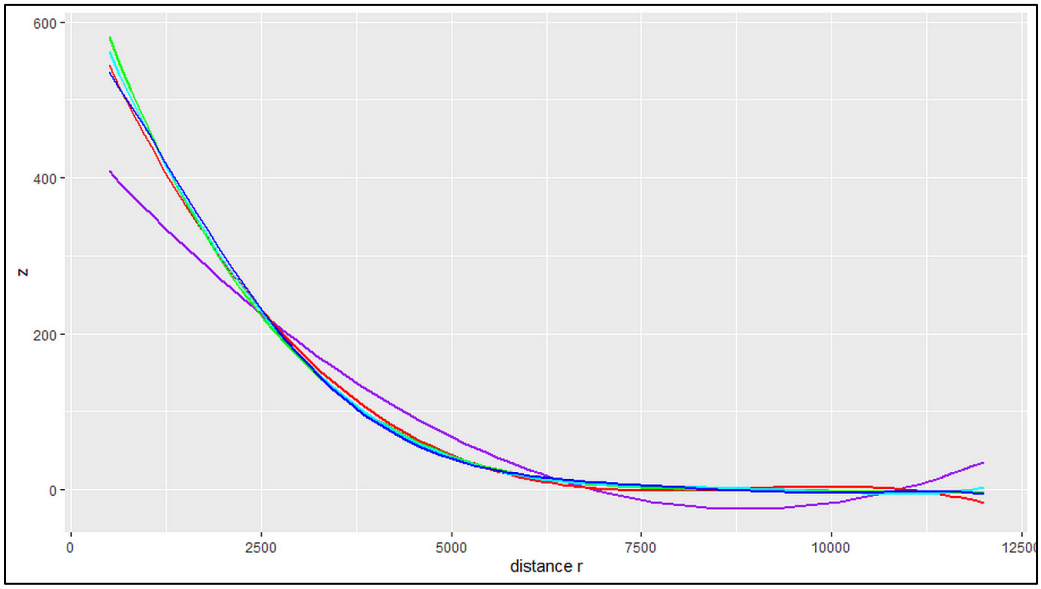

Figure 4. Polynomial curves of increasing degree (from 2 to 6) fitting the obtained set of data "distance to the center/cumulate uplift". Legend: 2nd, purple line; 3rd, red line; 4th, green line; 5th, cyan line; 6th, blue line.

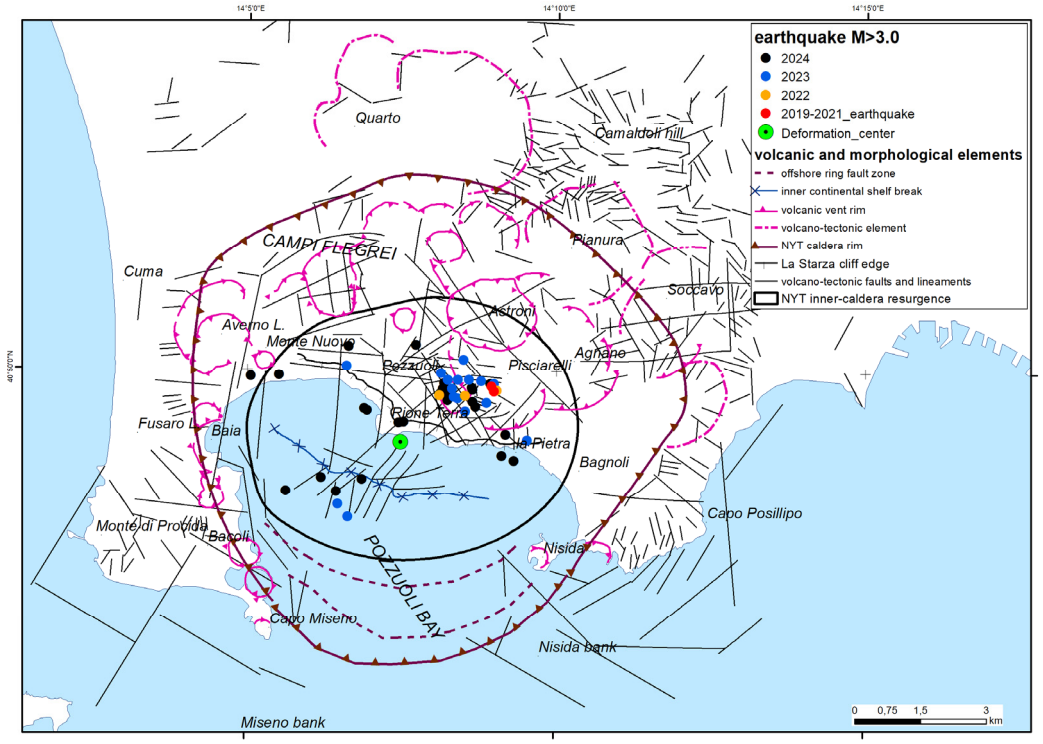

Figure 5. Datasets of volcano-tectonic faults and lineaments and earthquakes Md>3.0 occurred during 2019 to July 2024. Seismic events by INGV databases (see text for references).

4. Results

4.1. Ground Deformation Vertical and Horizontal Trends

The trends of vertical and horizontal ground deformation occurring on land in 2016-2021 are showed by EGMS Ortho Vertical and EGMS Ortho East/West datasets (Figures 6 and 7); no data is available about the ground deformation of the sea floor in the Pozzuoli Bay, even if deformation has involved also the sea submerged side of the caldera.

Preprints.org (www.preprints.org) | NOT PEER-REVIEWED | Posted: 11 September 2024 doi:10.20944/preprints202409.0809.v1

The ground deformation patterns referring to the 2016–2021 period show that the eastern sector of Campi Flegrei is characterized by eastward horizontal movements whereas the western sector is characterized by westward horizontal movements with maximum values in the caldera central area about 2 km west and east outside Pozzuoli (Figure 6). As we are considering only the E-W component of the horizontal movements, the velocity values strongly reduce along the N-S linear axis crossing through the center of the caldera deformation, located near Pozzuoli city center. Along this axis the N-S component of the horizontal movements is very high, and the E-W component is almost null due to the radial geometry of ground deformation. For this reason, considering the SAR acquisition geometry, the spatial pattern of horizontal velocity looks larger in the E to W direction.

The central area with negligible east-west displacement is characterized by maximum uplift rates (Figures 6 and 7). The vertical ground deformation of the Campi Flegrei during 2016–2021 period is mainly spatially symmetrical with a radial patter (Figure 7), with annual velocity varying from + 9 cm/yr in the central sector to zero in a strip between 6 and 7 km of distance from the deformation center. The areas external to the caldera rim, beyond 7 - 8 km from the center (Figure 6), are also characterized by small subsidence rates (- 1 to – 3 mm/year), that only locally may show lower rates up to – 14 mm/yr due to local subsidence or landslide processes.

The ground uplift is confined within a circle of about 7 km in diameter, corresponding to the caldera rim, and further amplified in the resurgent block [44,70,96], due to the control of the ring faults, bounding both the caldera and the resurgent block, on the ground deformation.

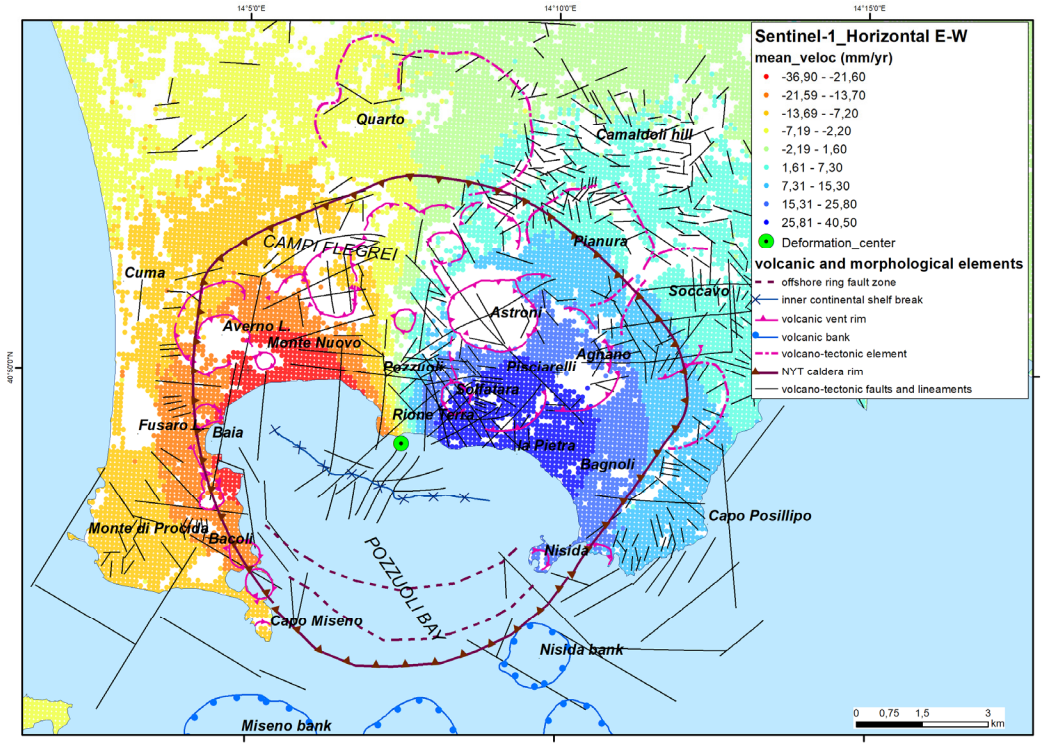

Figure 6. E-W horizontal component of ground deformation at Campi Flegrei during 2015-2021 derived by EGMS Ortho East/West dataset [97].

Preprints.org (www.preprints.org) | NOT PEER-REVIEWED | Posted: 11 September 2024 doi:10.20944/preprints202409.0809.v1

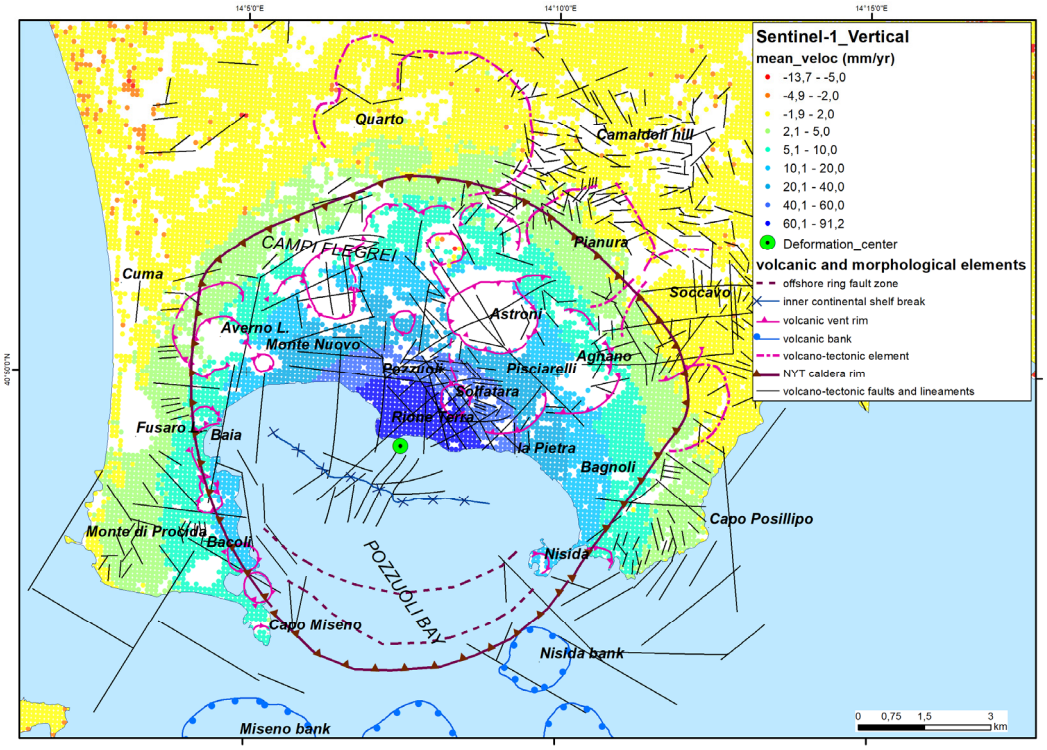

Figure 7. Vertical component of ground deformation at Campi Flegrei during 2015-2021 derived by EGMS Ortho Vertical dataset [97].

4.2. Vertical Ground Deformation Shape

The best-fit curve for vertical displacement component, obtained with the methodology described in sect. 3, is showed in Figure 8. It represents the theoretical radial and symmetric geometry of ongoing ground deformation along the vertical component and can be used to predict the best-fit expected value at a given distance from the deformation center for each point within the caldera.

The radial vertical deformation occurred in 2016-2021 period is characterized by a bell shape with a maximum in the center and values approaching zero radially moving away. The uplift values decline rapidly between 0.5 and 4.0 km of distance, then the reduction rate progressively slows up to about 6.0 km of distance and finally the uplift becomes very low up to 8-9 km from the center.

If we compare the recent normalized deformation pattern, referred only to uplift occurring during an inflation phase and obtained by Sentinel-1 ORTHO vertical DInSAR 2016-2021 data, with that of the last 120 years, derived by levelling measurements between 1905 and 1992 and 2000–2019 GNNS data performed in different unrest periods both in uplift and subsidence [93], we may obtain relevant information on ground deformation shape. Plots in Figure 9 shows a similar shape for the two plotted datasets. It is evident that unrest episodes at Campi Flegrei caldera (bradyseism phenomena) occurred in the last 120 years during both inflation and deflation episodes show the same ground deformation shape with a radial symmetry characterized by maximum uplift and subsidence vertical displacement values in the deformation center. Minor differences can be observed between N=0.23-0.95, where 1905-2019 curve shows values slightly higher than 2016-2021 curve and between N=0.01-0.22, where 1905-2019 curve shows values slightly lower than 2016-2021 curve. The crossing point between the two curves is located at about 4.0 km of distance from the deformation center, approximately at the border of the resurgence.

Preprints.org (www.preprints.org) | NOT PEER-REVIEWED | Posted: 11 September 2024 doi:10.20944/preprints202409.0809.v1

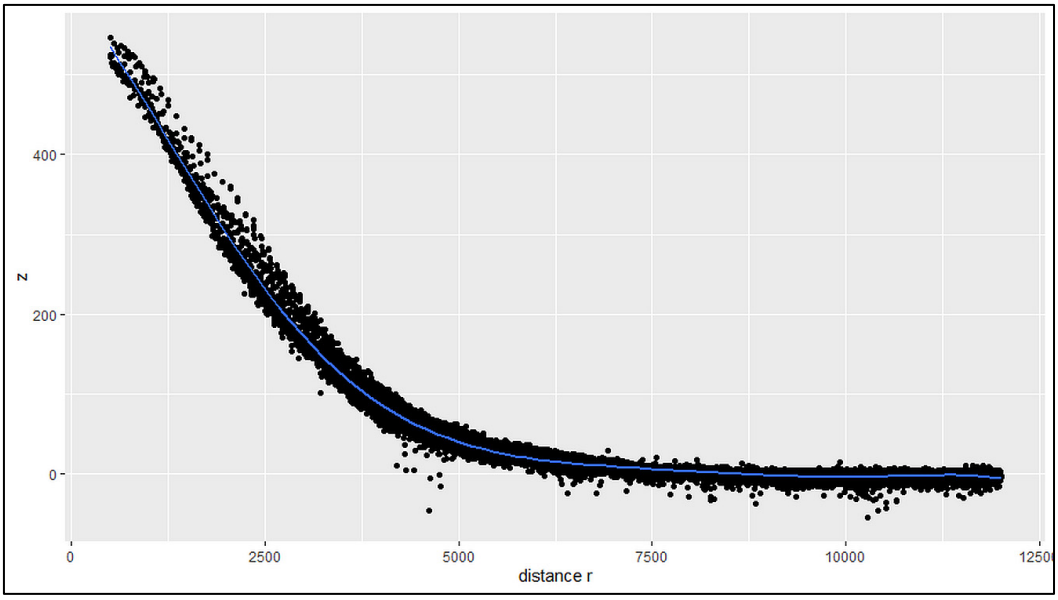

Figure 8. Polynomial curve (in blue) of 6th degree best fitting the obtained set of data of distance to the center ("r" measured in m) vs cumulate uplift during 2016-2021 ("N" measured in mm). Values of "r" lower than 500 m have not been considered for the calculation of the polynomial curve.

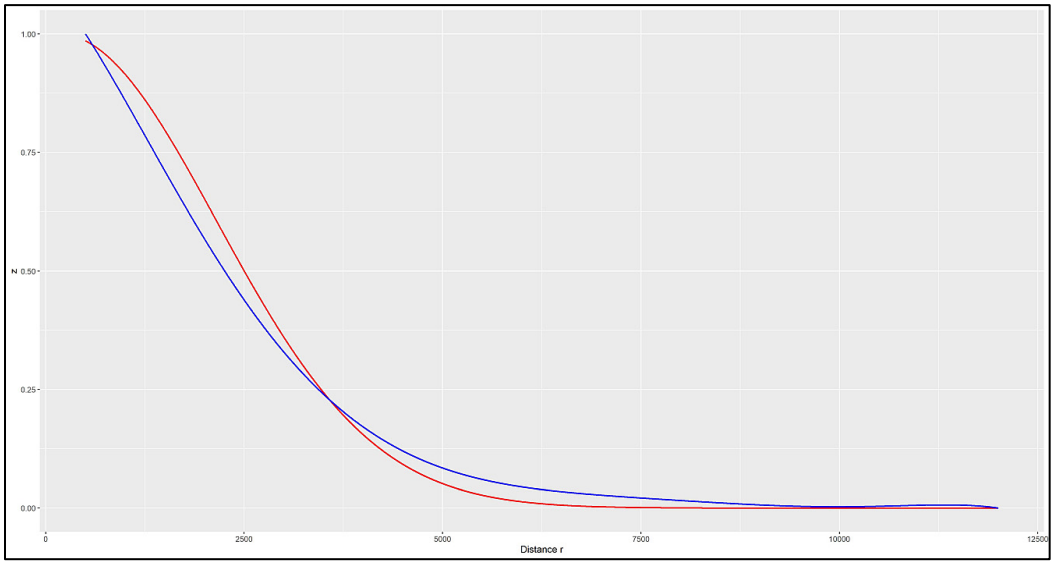

Figure 9. Plot normalized vertical ground deformation values (N) vs distance to the caldera deformation center (R). Comparison between curve by Vitale & Natale [93] (in red), derived by levelling measurements between 1905 and 1992 and 2000–2019 GPS data, and our curve, derived by Sentinel-1 ORTHO vertical DInSAR 2016-2021 data [97] (in blu).

4.3. Vertical Ground Deformation Anomalies

The maps of the differences for each point between the best-fit expected value at a given distance from the deformation center calculated with the polynomial curve and the observed (measured) values of vertical ground deformation allow to visualize the spatial distribution of anomalies between the predicted and actual uplift values.

In these maps (Figures 10 and 11), areas where the observed uplift is significantly higher than the predicted values are characterized by negative values and are mapped in yellow to red. Conversely, areas where the observed uplift is lower than what was predicted by the polynomial models are with positive values and are shaded in light to dark blue. The spatial representation of

 doi:10.20944/preprints202409.0809.v1

these anomalies provides relevant insights into the deformation second-order patterns and allows for a better understanding of the areas experiencing significant differences in uplift or subsidence.

Whitin the caldera area two main anomalies are well mapped: i) a negative values large sector is located between Baia to the west and Pozzuoli city center to the east; ii) a sector with high positive values is located between Monte Olibano, Solfatara and Bagnoli. These sectors with differences in uplift are separated by some lineaments: A) a well-marked SW-NE oriented line goes from deformation center to Pisciarelli and Agnano and separates sectors characterized by – 30 mm to + 30-45 mm of uplift anomaly (about 60-75 mm of difference in total); B) an ill-defined SSW-NNE oriented line between Bagnoli and La Pietra separates sectors characterized by + 15 mm to + 45 mm of uplift anomaly (about 30 mm of difference in total); C) a well-marked NW-SE oriented line goes from Baia to Fusaro Lake and separates sectors characterized by – 15 mm to + 15 mm of uplift anomaly (about 30mm of difference in total).

In Figure 10, the vertical ground deformation anomalies are compared with volcano-tectonic elements and faults. The lineament A falls within a sector crossed by several SW-NE, N-S and NW-SE faults and the differential uplift seems to be controlled by SW-NE fault set. The lineament B do not correspond to any mapped fault, while the lineament C seems to be crossed by N-S, E-W and NW-SE faults. Both B and C lineaments are parallel to the local orientation of the caldera rim.

In Figure 11, it can be seen a clear spatial correlation among 2019-2024 earthquake epicenters and uplift anomalies along lineament A between Pozzuoli and Bagnoli, while the earthquake epicenters near the lineament C are located in the sea, along faults located in the bay bottom.

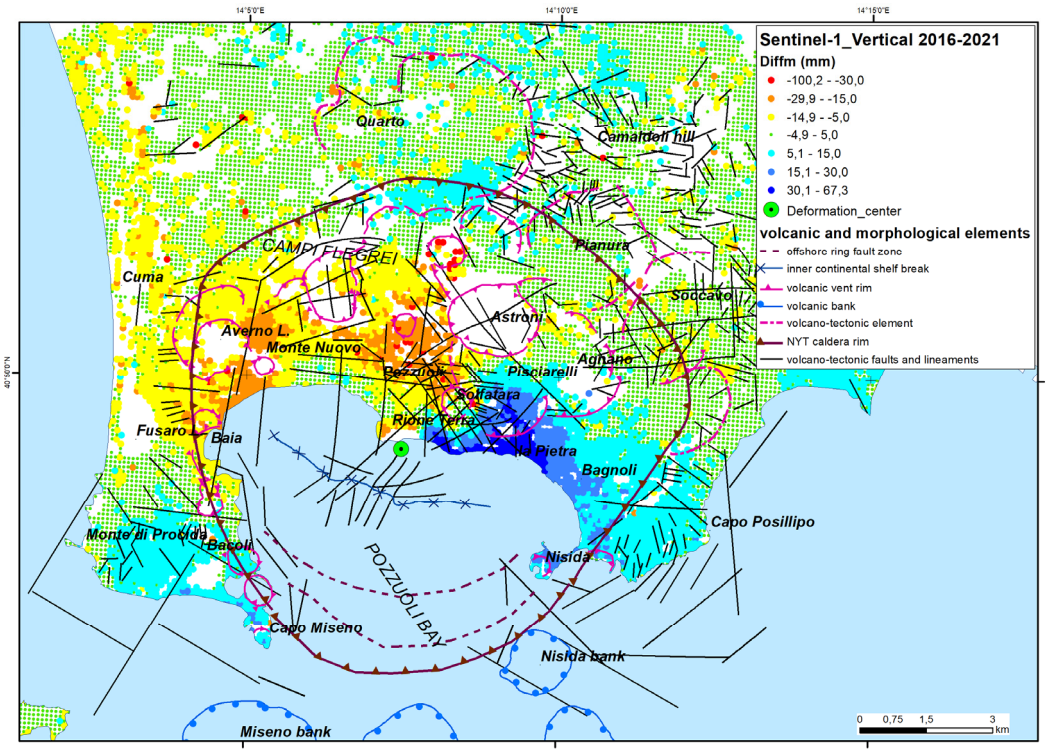

Figure 10. Vertical ground deformation anomalies compared with volcano-tectonic elements.

 doi:10.20944/preprints202409.0809.v1

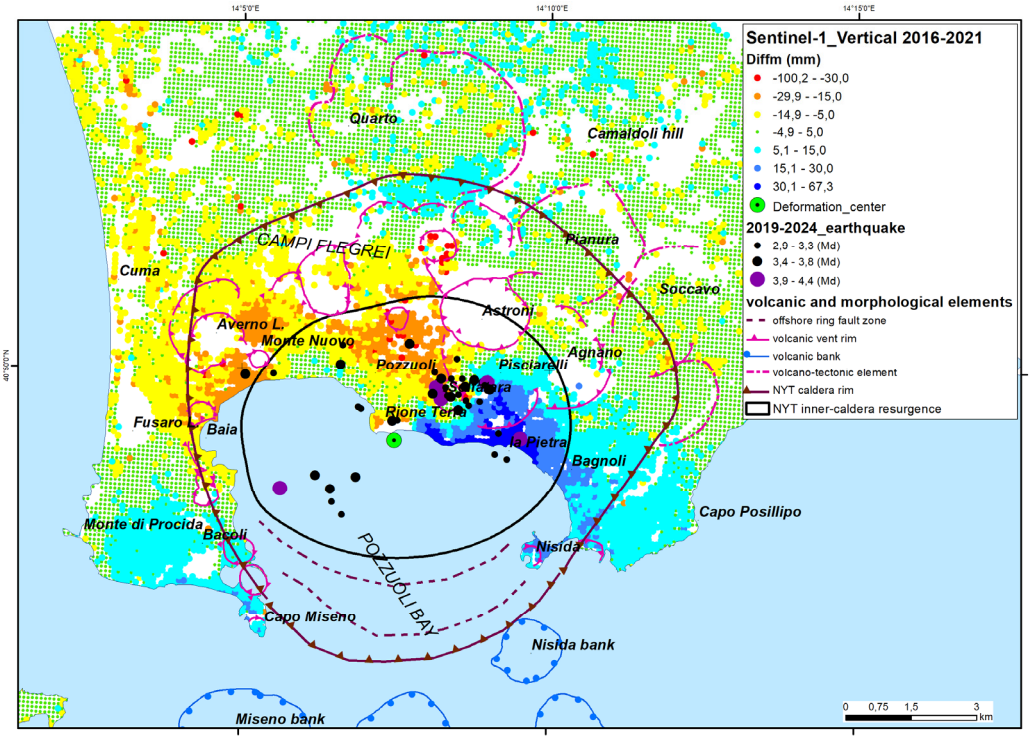

Figure 11. Vertical ground deformation anomalies compared with seismic events.

5. Discussion and Conclusions

Our results confirm that the overall, first order geometry of the vertical ground deformation pattern at Campi Flegrei is 'bell shaped', very concentrated in a small area [7,13,27,57] which likely corresponds to the resurgent block inside the caldera [44]. The vertical deformation we inferred in the analyzed period (2016-2021) is uplift, but it has been observed, from MT-InSAR, precision levellings and GPS measurements during the period 1905-2019, that also the subsidence in the area is perfectly specular to the uplift [57,98]. As shown by De Natale and Pingue [69] and De Natale et al. [70], the very constant shape of deformation pattern, both for uplift and for subsidence, as well as the large amount of deformation, is well explained by the presence of a central zone bordered by ring fault. Such structure is likely to be represented by the central resurgent block recently well evidenced by Rolandi et al. [44], and already hypothesized and supported by the combined observations of seismicity and ring faults at sea by Sacchi et al. [31,32].

However, our work also identifies, for the first time, some peculiar deviations (anomalies in uplift) from such a 'bell shaped' pattern, which has been characterized by a best fitting polynomial. Fitting the available data to a specific inflation/deflation source model goes beyond the scope of this work, so we do not elaborate a specific model.

The deviations from the best fitting curves are significantly nonrandom. The most prominent lineament is the sharp change between negative and positive anomalies, separated by a roughly NE-SW line slightly East of the Rione Terra and crossing Solfatara crater. This line closely resembles the tectonic lineation connecting La Pietra to the western Agnano plain bounding faults [68,99,100], and most of the seismicity, particularly the largest magnitude earthquakes, appears located along or very close to this line. The clustering of seismicity along the separation line between negative and positive anomalies strongly suggests this feature is linked to coseismic displacements. We recall that very shallow seismicity, typical of Campi Flegrei earthquakes, can produce measurable coseismic displacement, from some mm to some cm, even with magnitude as low as 3-4. The example of the 2017 Casamicciola (Ischia Island) M=4.0 earthquake is worthy of note: it caused more than 4 cm of subsidence in the hanging wall. The depth of the Casamicciola earthquake was about 2 km, a depth very similar to the Campi Flegrei earthquakes [45,68,101,102].

 doi:10.20944/preprints202409.0809.v1

As pointed out in several papers [68,103,104] Campi Flegrei earthquakes have dominant normal fault mechanisms. The normal faulting earthquakes at Campi Flegrei, mainly clustered around the ring faults bordering the resurgent block, are characterized by movements which are opposite to the dominant source of static deformation (generating uplift of the central block), anyway representing only a minimum fraction of the total deformation [104,105]. Such a feature of the seismicity is in agreement with the present observations, in which the occurrence of earthquakes produces a slight subsidence of part of the most uplifted resurgent block, with respect to the areas external to the main bordering faults.

The detected alignment A, which sharply separates positive and negative vertical deformation anomalies, is then likely to correspond to a main seismic fault zone, which can give the highest magnitude earthquakes in the area.

It is interesting to note that earthquakes occurred before 2020 (Figure 5), when the total uplift was lower than today, were much more concentrated around this structure. This is in agreement with the hypothesis that this could be the main seismogenic structure in the area, and that other structural features, located more distant from the center of uplift, have been progressively activated by a progressive enlargement of the critical stress threshold, which is a direct consequence of the progressive increase of the ground uplift (e.g. [106]). Such a main structural feature in the area possibly represents also the most likely zone for possible vent opening in a future eruptive scenario: phreatic and/or magmatic. In particular, the small area included among Rione Terra, Solfatara-Pisciarelli and La Pietra appears to be the most anomalous one, characterized by the sharp change in the sign of the residual displacement and by the most prominent anomalies, indicating a local relative subsidence.

The procedure adopted for the analysis of anomalies in vertical ground deformations detected by the MT-InSAR Sentinel 1 datasets during the unrest phase of the Phlegraean caldera shows that differential ground movements (at mm and cm scales) related to seismic structures that have not yet been fully activated can be recognized in the early stages of increased ground deformation and seismicity, if appropriately filtered and analyzed.

The spatial distribution of earthquakes occurring since 2022 and their focal mechanisms clearly demonstrate that ground deformation anomalies are, in the case study, detectable from the analysis of deformations measured in 2015-2021. By identifying these ground deformation anomalies, it is possible to refine models and improve the accuracy of future predictions.

Author Contributions: Conceptualization, F.M. and G.DN.; methodology, F.M. and A.C.; software, A.C.; validation, F.M. and G.DN.; formal analysis, F.M. and A.C.; investigation, F.M. and G.DN.; resources, F.M.; writing—original draft preparation, F.M., A.C. and G.DN.; writing—review and editing, F.M. and G.DN.; visualization, F.M. and A.C. All authors have read and agreed to the published version of the manuscript.

Funding: This research received no external funding.

Data Availability Statement: European Union's Copernicus Land Monitoring Service data, https://doi.org/10.2909/943e9cbb-f8ef-4378-966c-63eb761016a9.

Acknowledgments: This publication has been prepared using European Union's Copernicus Land Monitoring Service information; DOI: https://doi.org/10.2909/943e9cbb-f8ef-4378-966c-63eb761016a9.

Conflicts of Interest: The authors declare no conflicts of interest.

References

1. Galetto, F., Acocella, V. & Caricchi, L. (2017) Caldera resurgence driven by magma viscosity contrasts. Nat Commun 8, 1750. https://doi.org/10.1038/s41467-017-01632-y
2. Marsh, B. D. (1984) On the mechanics of caldera resurgence. J. Geophys. Res. 89, 8245–8251.
3. Kennedy, B., Wilcock, J. & Stix, J. (2012) Caldera resurgence during magma replenishment and rejuvenation at Valles and Lake City calderas. Bull. Volcanol. 74, 1833–1847.
4. De Silva, S. L., Mucek, A. E., Gregg, P. M. & Pratomo, I. (2015) Resurgent Toba—field, chronologic, and model constraints on time scales and mechanisms of resurgence at large calderas. Front. Earth Sci. 3, 25.

5. De Natale, G., Pingue, F., Allard, P., Zollo, A., 1991. Geophysical and geochemical modelling of the 1982-1984 unrest phenomena at Campi Flegrei caldera (southern Italy). Journal of Volcanology and Geothermal Research, 1991, 48(1-2), pp. 199–222.
6. Hurwitz S, Christiansen LB, Hsieh PA (2007) Hydrothermal fluid flow and deformation in large calderas: Inferences from numerical simulations. Journal of Geophysical Research 112: B02206, 16 pp, doi:10.1029/2006JB004689
7. Troise, C., De Natale, G., Schiavone, R., Somma, R., Moretti, R., 2019. The Campi Flegrei caldera unrest: Discriminating magma intrusions from hydrothermal effects and implications for possible evolution. Earth-Science Reviews, 188, pp. 108–122
8. Acocella V (2019) Bridging the gap from caldera unrest to resurgence. Front. Earth Sci. 7:173
9. Newhall CG, Dzurisin D (1988) Historical unrest at large calderas of the world. U.S. G.P.O., Bulletin 1855, 2 v. 1108
10. Phillipson G, Sobradelo R, Gottsmann J (2013) Global volcanic unrest in the 21st century: an analysis of the first decade. J Volcanol Geotherm Res 264:183–196
11. Acocella V, Di Lorenzo R, Newhall C, Scandone R (2015) An overview of recent (1988 to 2014) caldera unrest: knowledge and perspectives. Rev Geophys 53:896–955
12. Charlton, D., Kilburn, C. & Edwards, S. Volcanic unrest scenarios and impact assessment at Campi Flegrei caldera, Southern Italy. J Appl. Volcanol. 9, 7 (2020). https://doi.org/10.1186/s13617-020-00097-x
13. Barberi F, Corrado G, Innocenti F, Luongo G (1984) Phlegraean fields 1982-1984: brief chronicle of a volcano emergency in a densely populated area. Bull Volcanol 47:175–185
14. Johnston D, Scott BJ, Houghton B, Paton D, Dowrick DJ, Villamor P, Savage J (2002) Social and economic consequences of historic caldera unrest at the Taupo volcano, New Zealand and the management of future episodes of unrest. Bull N Z Soc Earthq Eng 35(4):215–230
15. Kuester I, Forsyth S (1985) Rabaul eruption risk: population awareness and preparedness survey. Disasters. 9:179–182
16. Benson C (2006) Volcanoes and the economy. In: Marti J, Ernst GGJ (eds) Volcanoes and the environment. Cambridge University Press, Cambridge, pp 440–467
17. INGV, 2024. Bollettino di Sorveglianza Campi Flegrei, mese di Giugno 2024. INGV, Sezione di Napoli – Osservatorio Vesuviano, 51 pp. https://www.ov.ingv.it/index.php/monitoraggio-e-infrastrutture/bollettini-tutti/bollett-mensili-cf/anno-2024-3/1652-bollettino-mensile-campi-flegrei-2024-06/file
18. Pappalardo, L., Civetta, L., D'Antonio, M., Deino, A., Di Vito, M., Orsi, G., Carandente, A., de Vita, S., Isaia, R., Piochi, M. (1999). Chemical and Sr-isotopical evolution of the Phlegraean magmatic system before the Campanian Ignimbrite and the Neapolitan Yellow Tuff eruptions. Journal of Volcanology and Geothermal Research, 91, 2–4, 141-166, https://doi.org/10.1016/S0377-0273(99)00033-5.
19. Scarpati, C., Sparice, D., Perrotta, A., (2014). A crystal concentration method for calculating ignimbrite volume from distal ash-fall deposits and a reappraisal of the magnitude of the Campanian Ignimbrite. J. Volcanol. Geotherm. Res. 280, 67–75
20. Orsi, G., De Vita, S., Di Vito, M. (1996). The restless, resurgent Campi Flegrei nested caldera (Italy): constraints on its evolution and configuration. Journal of Volcanology and Geothermal Research, 74(3-4), 179-214.
21. Rosi, M., Vezzoli, L., Aleotti, P., De Censi, M. (1996). Interaction between caldera collapse and eruptive dynamics during the Campanian Ignimbrite eruption, Phlegraean Fields, Italy. Bull Volcanol 57, 541–554. https://doi.org/10.1007/BF00304438
22. De Vivo, B., Rolandi, G., Gans, P. B., Calvert, A., Bohrson, W. A., Spera, F. J., Belkin, H.E. (2001). New constraints on the pyroclastic eruptive history of the Campanian volcanic plain (Italy). Mineralogy and Petrology, 73, 47–65. doi: 10.1007/s007100170010
23. Deino A L, Orsi G, de Vita S, Piochi M. (2004). The age of the Neapolitan Yellow Tuff caldera-forming eruption (Campi Flegrei caldera – Italy) assessed by 40Ar/39Ar dating method. Journal of Volcanology and Geothermal Research,133, 1–4, 157-170, https://doi.org/10.1016/S0377-0273(03)00396-2.
24. Orsi, G., D'Antonio, M., de Vita, S., Gallo, G., 1992. The Neapolitan Yellow Tuff, alarge-magnitude trachytic phreatoplinian eruption: eruptive dynamics, magma withdrawal and caldera collapse. J. Volcanol. Geotherm. Res. 53, 275–287.

25. Wohletz, K., Orsi, G., De Vita, S. (1995). Eruptive mechanisms of the Neapolitan Yellow Tuff interpreted from stratigraphic, chemical, and granulometric data. Journal of Volcanology and Geothermal Research, 67(4), 263-290.
26. Perrotta, A., Scarpati, C., Luongo, G., & Morra, V. (2006). The Campi Flegrei caldera boundary in the city of Naples. In Developments in Volcanology, Editor(s): B. De Vivo, Elsevier, Volume 9, 85-96, https://doi.org/10.1016/S1871-644X(06)80019-7
27. De Natale G., Troise C., Mark D., Mormone A., Piochi M., Di Vito M.A., Isaia R., Carlino S., Barra D., Somma R. (2016) The Campi Flegrei Deep Drilling Project (CFDDP): New insight on caldera structure, evolution and hazard implications for the Naples area (Southern Italy). Geochemistry, Geophysics, Geosystems, 17 (12), pp. 4836 – 4847; DOI: 10.1002/2015GC00618
28. De Natale, G., Rolandi, G., Kilburn, C.R.J., Troise, C., Somma, R., Di Vincenzo, G., Rolandi, R., Woo, J., Cole, P.D., 2024. The Campanian Ignimbrite of southern Italy: a fissure eruption or caldera-forming event? Earth Plan. Sci. Lett., submitted.
29. Rolandi, G., De Natale G., Kilburn, C.R.J. et al., 2020. The 39 ka Campanian Ignimbrite eruption: new data on source area in the Campanian Plain," in Vesuvius, Campi Flegrei, and Campanian volcanism, Chapt. 8, B. Vivo, H. E. Belkin, and G. Rolandi, Eds., pp. 175–205, Elsevier
30. Orsi G., Civetta L., Del Gaudio C., de Vita S., Di Vito M.A., Isaia R., Petrazzuoli S.M., Ricciardi G.P., Ricco C. (1999). Short-term deformations and seismicity in the resurgent Campi Flegrei caldera (Italy): an example of active block-resurgence in a densely populated area. Journal of Volcan. And Geoth. Res. (91) 415-451.
31. Sacchi, M., Pepe, F., Corradino, M., Insinga, D.D., Molisso, F., Lubritto C., 2014. The Neapolitan 1217 Yellow Tuff caldera offshore the Campi Flegrei: stratal architecture and kinematic reconstruction 1218 during the last 15 ky. Mar. Geol. 354, 5-33
32. Sacchi, M., Matano, F., Molisso, F., Passaro, S., Caccavale, M., Di Martino, G., Guarino, A., Innangi, S., Tamburrino, S., Tonielli, R., Vallefuoco, M., 2020. Geological framework of the Bagnoli–Coroglio coastal zone and continental shelf, Pozzuoli (Napoli) Bay. Chem. Ecol., 36, 529–549. https://doi.org/10.1080/02757540.2020.1735374
33. Di Vito, M.A., Isaia, R., Orsi, G., Southon, J. D., De Vita, S., D'Antonio, M., Pappalardo L., Piochi, M. (1999). Volcanism and deformation since 12,000 years at the Campi Flegrei caldera (Italy). Journal of Volcanology and Geothermal Research, 91(2-4), 221-246.
34. Isaia, R., Marianelli, P., Sbrana, A. (2009). Caldera unrest prior to intense volcanism in Campi Flegrei (Italy) at 4.0 ka BP: Implications for caldera dynamics and future eruptive scenarios. Geophysical Research Letters 36 (21)
35. Di Renzo V., Arienzo I., Civetta L., D'Antonio M., Tonarini S., Di Vito M.A., Orsi G. (2011). The magmatic feeding system of the Campi Flegrei caldera: Architecture and temporal evolution. Chemical Geology, 281, 3–4, 227-241, https://doi.org/10.1016/j.chemgeo.2010.12.010.
36. Smith, V. C., Isaia, R., Pearce, N. J. G. (2011). Tephrostratigraphy and glass compositions of post-15 kyr Campi Flegrei eruptions: implications for eruption history and chronostratigraphic markers. Quaternary Science Reviews, 30(25-26), 3638-3660.
37. Lirer L, Luongo G, Scandone R (1987) On the volcanological evolution of Campi Flegrei. EOS 68(16): 226–233.
38. De Vita, S., Orsi, G., Civetta, L., Carandente, A., D'Antonio, M., Deino, A., di Cesare, T., Di Vito, M.A., Fisher, R.V., Isaia, R., Marotta, E., Necco, A., Ort, M., Pappalardo, L., Piochi, M., Southon, J. (1999). The Agnano–Monte Spina eruption (4100 years BP) in the restless Campi Flegrei caldera (Italy). Journal of Volcanology and Geothermal Research, 91, 2–4, 269-301, https://doi.org/10.1016/S0377-0273(99)00039-6.
39. Dellino, P., Dioguardi, F., Isaia, R., Sulpizio, R., Mele, D. 2021. The impact of pyroclastic density currents duration on humans: The case of the AD 79 eruption of Vesuvius. Scientific Reports 11(1), 49-59. https://doi.org/10.1038/s41598-021-84456-7.
40. Di Vito, M., Lirer, L., Mastrolorenzo, G., & Rolandi, G. (1987). The 1538 Monte Nuovo eruption (Campi Flegrei, Italy). Bulletin of Volcanology, 49, 608-615.
41. Di Vito, M., Acocella, V., Aiello, G. Barra D, Battaglia M, Carandente A, Del Gaudio C, de Vita S, Ricciardi G P., Ricco C, Scandone R & Terrasi F. (2016). Magma transfer at Campi Flegrei caldera (Italy) before the 1538 AD eruption. Sci Rep 6, 32245 (2016). https://doi.org/10.1038/srep32245

42. Piochi, M., Mastrolorenzo, G., Pappalardo, L. (2005). Magma ascent and eruptive processes from textural and compositional features of Monte Nuovo pyroclastic products, Campi Flegrei, Italy. Bulletin of Volcanology. 67. 663-678. 10.1007/s00445-005-0410-1.
43. Guidoboni E., Ciuccarelli C., 2011. The Campi Flegrei caldera: historical revision and new data on seismic crises, bradyseisms, the Monte Nuovo eruption and ensuing earthquakes (twelfth century 1582 AD). Bulletin of Volcanology, 73, 655–677. https://doi.org/10.1007/s00445-010-0430-3
44. Rolandi, G., Troise, C., Sacchi, M., di Lascio, M., De Natale, G. (2024). The 1538 eruption at Campi Flegrei resurgent caldera: implications for future unrest and eruptive scenarios. EGUsphere Preprint repository, https://doi.org/10.5194/egusphere-2024-2035
45. De Natale, G., Troise, C., Pingue, F., Mastrolorenzo, G., Pappalardo, L., Battaglia, M., Boschi, E. (2006). The Campi Flegrei caldera: Unrest mechanisms and hazards. Geol. Soc. London Spec. Pubi., 269 (1), 10.1144/GSL.SP.2006.269.01.0
46. Vitale S, Isaia R (2014) Fractures and faults in volcanic rocks (Campi Flegrei, Southern Italy): insight into volcano-tectonic processes. Int J Earth Sci 103:801–819
47. Natale J, Camanni G, Ferranti L, Isaia R, Sacchi M, Spiess V, Steinmann L, Vitale S (2022) Fault systems in the ofshore sector of the Campi Flegrei caldera (southern Italy): implications for nested caldera structure, resurgent dome, and volcano-tectonic evolution. J Struct Geol 163:104723. https://doi.org/10.1016/j.jsg.2022.104723
48. Steinmann L, Spiess V, Sacchi M., 2016. The Campi Flegrei caldera (Italy): formation and evolution in interplay with sea-level variations since the Campanian Ignimbrite eruption at 39 ka. J Volcanol Geotherm Res., 327, 361–374.
49. Steinmann L, Spiess V, Sacchi M., 2018. Post-collapse evolution of a coastal caldera system: Insights from a 3D multichannel seismic survey from the Campi Flegrei caldera (Italy). J Volcanol Geotherm Res., 349, 83–98.
50. Isaia R, Vitale S, Di Giuseppe MG, Iannuzzi E, Tramparulo FDA, Troiano A (2015) Stratigraphy, structure and volcano-tectonic evolution of Solfatara maar diatreme (Campi Flegrei, Italy). Geol Soc Am Bull 127:1485–1504
51. Rosi, M., Sbrana, A., 1987. Phlegrean fields. Quaderni de la ricerca scientifica 9 (114).
52. Orsi G, D'Antonio M, Civetta L (eds.) (2022) Campi Flegrei. Active volcanoes of the world, Springer, Berlin, Heidelberg, pp 201–217
53. Parascandola A (1947) I fenomeni bradisismici del Serapeo di Pozzuoli. Stabilmento tipografico G. Genovese
54. Morhange C, Bourcier M, Laborel J, Giallanella C, Goiran JP, Crimaco L, Vecchi L (1999) New data on historical relative sea level movements in Pozzuoli, Phlaegrean Fields, southern Italy. Phys Chem Earth Part A 24:349–354
55. Bellucci F, Woo J, Kilburn CRJ, Rolandi G (2006) Mechanisms of activity and unrest at large calderas. Geol Soc Lond, Special Publications. 269:141–158
56. Amoruso A, Crescentini L, Sabbetta I (2014) Paired deformation sources of the Campi Flegrei caldera (Italy) required by recent (1980–2010) deformation history. J Geophys Res: Solid Earth 119:858–879.
57. Battaglia M, Troise C, Obrizzo F, Pingue F, De Natale G (2006) Evidence for fluid migration as the source of deformation at Campi Flegrei caldera (Italy). Geophys Res Lett 33:L01307
58. D'Auria L, Pepe S, Castaldo R, Giudicepietro F, Macedonio G, Ricciolino P, Tizzani P, Casu F, Lanari R, Manzo M, Martini M, Sansosti E, Zinno I (2015) Magma injection beneath the urban area of Naples: a new mechanism for the 2012–2013 volcanic unrest at Campi Flegrei caldera. Sci Rep 5(1):1–11
59. Lima A, De Vivo B, Spera FJ, Bodnar RJ, Milia A, Nunziata C, Belkin HE, Cannatelli C (2009) Thermodynamic model for uplift and deflation episodes (Bradyseism) associated with magmatic hydrothermal activity at the Campi Flegrei active volcanic center (Italy). Earth Sci Rev 97:44–58
60. Macedonio G, Giudicepietro F, D'Auria L, Martini M (2014) Sill intrusion as a source mechanism of unrest at volcanic calderas. J Geophys Res Solid Earth 119:3986–4000
61. Todesco M, Neri A, Esposti Ongaro T, Papale P, Rosi M (2006) Pyroclastic flow dynamics and hazard in a caldera setting: application to Phlegrean Fields (Italy). Geochem Geophys Geosyst 7:Q11003
62. Woo JYL, Kilburn CRJ (2010) Intrusion and deformation at Campi Flegrei, southern Italy: sills, dikes, and regional extension. J Geophys Res 115:B12210

63. Cannatelli C., Spera F.J., Bodnar R.J., Lima A., De Vivo B. (2020) Ground movement (bradyseism) in the Campi Flegrei volcanic area: a review. Editor(s): Benedetto De Vivo, Harvey E. Belkin, Giuseppe Rolandi, Vesuvius, Campi Flegrei, and Campanian Volcanism, Elsevier, 2020, 407-433, https://doi.org/10.1016/B978-0-12-816454-9.00015-8.
64. Del Gaudio, C., Aquino, I., Ricciardi, G. P., Ricco, C. and Scandone R. (2010) Unrest episodes at Campi Flegrei: A reconstruction of vertical ground movements during 1905–2009, J. Volcanol. Geotherm. Res., 195(1), 48–56; 10.1016/j.jvolgeores.2010.05.014
65. Barberi F., Cassano E., La Torre P., Sbrana, A. (1991) Structural evolution of Campi Flegrei caldera in light of volcanological and geophysical data. Journal of Volcanology and Geothermal Research, 48, 1–2, 1991, 33-49, https://doi.org/10.1016/0377-0273(91)90031-T.
66. Falanga, M., Aquino, I., De Lauro, E., Petrosino, S., & Ricco, C. (2023). New insights on ground deformation at Campi Flegrei caldera inferred from kinematics and dynamics investigation of borehole tilt. Earth and Space Science, 10(3), e2022EA002702, doi: doi.org/10.1029/2022EA002702.
67. Kilburn, C.R.J., De Natale, G., Carlino, S. (2017) Progressive approach to eruption at Campi Flegrei caldera in southern Italy. Nature Communications, 8, 15312.
68. Scotto di Uccio, F., Lomax, A., Natale, J., Muzellec, T., Festa, G., Nazeri, S., et al. (2024). Delineation and fine-scale structure of fault zones activated during the 2014–2024 unrest at the Campi Flegrei caldera (Southern Italy) from high-precision earthquake locations. Geophysical Research Letters, 51, e2023GL107680. https://doi.org/10.1029/2023GL107680
69. De Natale, G., Pingue F. 1993. "Ground Deformations in Collapsed Caldera Structures." Journal of Volcanology and Geothermal Research 57: 19–38. doi:10.1016/0377-0273(93)90029-Q.
70. De Natale G, Petrazzuoli SM, Pingue F (1997) The effect of collapse structures on ground deformations in calderas. Geophys Res Lett 24(13):1555–1558
71. Iuliano S., Matano F., Caccavale M., Sacchi M., 2015. Annual rates of ground deformation (1993-2010) at Campi Flegrei, Italy, revealed by Persistent Scatterer Pair (PSP) - SAR Interferometry. International Journal of Remote Sensing, 36, 24, 6160-6191. doi: 10.1080/01431161.2015.1111541.
72. Ricco, C.; Petrosino, S.; Aquino, I.; Del Gaudio, C.; Falanga, M. 2019. Some Investigations on a Possible Relationship between Ground Deformation and Seismic Activity at Campi Flegrei and Ischia Volcanic Areas (Southern Italy). Geosciences, 9, 222. https://doi.org/10.3390/geosciences9050222
73. Ortolani F., Pagliuca S., 1988. Principali effetti superficiali del bradisismo di Pozzuoli (Campania) e relazioni con le caratteristiche geologico-tecniche dei terreni. Mem. Soc. Geol. It., 41, 963-968.
74. Pingue F., Petrazzuoli S.M., Obrizzo F., Tammaro U., De Martino P., Zuccaro G., 2011. Monitoring system of buildings with high vulnerability in presence of slow ground deformations (The Campi Flegrei, Italy, case). Measurement, 44, 9, 1628-1644, https://doi.org/10.1016/j.measurement.2011.06.015.
75. Somma R, Iuliano S, Matano F, Molisso F, Passaro S, Sacchi M, Troise C, De Natale G (2016) High-resolution morpho-bathymetry of Pozzuoli Bay, southern Italy. J Maps 12:222–230
76. Bottiglieri, M., M. Falanga, U. Tammaro, P. De Martino, F. Obrizzo, C. Godano, F. Pingue. 2010. "Characterization of GPS time series at the Neapolitan volcanic area by statistical analysis." Journal of Geophysical Research: 115 (B10416): 1-5. doi: 10.1029/2009JB006594
77. De Martino P, Dolce M, Brandi G, Scarpato G, Tammaro U (2021) The Ground Deformation History of the Neapolitan Volcanic Area (Campi Flegrei Caldera, Somma-Vesuvius Volcano, and Ischia Island) from 20 years of continuous GPS observations (2000–2019). Rem Sens 13:2725
78. Hanseen, R. F. 2001. Radar Interferometry, Data Interpretation and Error Analysis. Kluwer Academic Publishers. ISBN 978-0792369455
79. Hooper, A., H. Zebker, P. Segall, B. Kampes. 2004. "A new method for measuring deformation on volcanoes and other natural terrains using InSAR persistent scatterers." Geophysical Research Letters 31 (L23611): 1-5. doi: 10.1029/2004GL021737
80. Vilardo, G.; Isaia, R.; Ventura, G.; De Martino, P.; Terranova, C. InSAR Permanent Scatterer analysis reveals fault re-activation during inflation and deflation episodes at Campi Flegrei caldera. Remote Sens. Environ. 2010, 114, 2373–2383. doi: 10.1016/j.rse.2010.05.014
81. Gabriel, A.K., R.M. Goldstein, H.A. Zebker, 1989. "Mapping small elevation changes over large areas: Differential radar interferometry." Journal of Geophysical Research 94: 9183–9191. doi: 10.1029/JB094iB07p09183

82. Massonnet, D., K.L. Feigl. 1998. “Radar interferometry and its application to changes in the Earth's surface.” Reviews of Geophysics 36: 441–500. doi: 10.1029/97RG03139
83. Matano, F; 2019. Analysis and Classification of Natural and Human-Induced Ground Deformations at Regional Scale (Campania, Italy) Detected by Satellite Synthetic-Aperture Radar Interferometry Archive Datasets. Remote Sensing, Volume: 11, Issue: 23, Article Number: 2822, DOI: 10.3390/rs11232822
84. Vilardo, G., G. Ventura, C. Terranova, F. Matano, S. Nardò. 2009. “Ground deformation due to tectonic, hydrothermal, gravity, hydrogeological and anthropic processes in the Campania Region (Southern Italy) from Permanent Scatterers Synthetic Aperture Radar Interferometry.” Remote Sensing of Environment 113: 197–212. doi:10.1016/j.rse.2008.09.007
85. Crosetto, M., Solari, L., Balasis-Levinsen, J., Bateson, L., Casagli, N., Frei, M., Oyen, A., Moldestad, D.A., Mróz, M., 2021. Deformation monitoring at European Scale: The Copernicus Ground Motion Service. In Proceedings of the International Archives of the Photogrammetry, Remote Sensing and Spatial Information Science. XXIV ISPRS Congress 2021; Vol. XLIII-b3-2, pp. 141–146.
86. Shahbazi, S., Crosetto, M., Barra, A., 2022. Ground Deformation Analysis Using Basic Products of the Copernicus Ground Motion Service. In Proceedings of the International Archives of the Photogrammetry, Remote Sensing and Spatial Information Sciences, XXIV ISPRS Congress, 43, 6–11.
87. Ferretti, A., C. Prati, and F. Rocca. 2001. “Permanent Scatterers in SAR Interferometry.” IEEE Transactions on Geoscience and Remote Sensing 39: 8–20. doi:10.1109/36.898661.
88. Berardino, P., G. Fornaro, R. Lanari, and E. Sansosti. 2002. “A New Algorithm for Surface Deformation Monitoring Based on Small Baseline Differential SAR Interferograms.” IEEE Transactions on Geoscience and Remote Sensing 40: 2375–2383. doi:10.1109/TGRS.2002.803792.
89. Ferretti, A., Fumagalli, A., Novali, F., Prati, C., Rocca, F., Rucci, A., 2011. A new algorithm for processing interferometric data-stacks: SqueeSAR. IEEE Transactions on Geoscience and Remote Sensing, 49(9), pp. 3460–3470, 5765671
90. Iannaccone G, Guardato S, Donnarumma GP, De Martino P, Dolce M, Macedonio G, Chierici F, Beranzoli L (2018) Measurement of seafloor deformation in the marine sector of the Campi Flegrei caldera (Italy). J Geophys Res: Solid Earth 123:66–83
91. Vitale S., Natale J. (2023) Combined volcano-tectonic processes for the drowning of the Roman western coastal settlements at Campi Flegrei (southern Italy). Earth, Planets and Space, 75, 38, https://doi.org/10.1186/s40623-023-01795-7
92. Ricciolino P., Lo Bascio D., Esposito R. (2024). GOSSIP - Database sismologico Pubblico INGV-Osservatorio Vesuviano. Istituto Nazionale di Geofisica e Vulcanologia (INGV). https://doi.org/10.13127/gossip
93. Natale J., Vitale S., Repola L., Monti L., Isaia R. (2024) Geomorphic analysis of digital elevation model generated from vintage aerial photographs: A glance at the pre-urbanization morphology of the active Campi Flegrei caldera. Geomorphology 460, 109267; https://doi.org/10.1016/j.geomorph.2024.109267
94. Natale J. (2024) Geomorphic analysis of digital elevation model generated from vintage aerial photographs: A glance at the pre-urbanization morphology of the active Campi Flegrei caldera. OSF Data Repository. doi 10.17605/OSF.IO/TX9HV
95. Natale J., Ferranti L., Isaia R., Marino C., Sacchi M., Spiess V., Steinmann L., Vitale S. (2022) Integrated on-land-offshore stratigraphy of the Campi Flegrei caldera: new insights into the volcano-tectonic evolution in the last 15 kyr Basin Res., 34 (2), pp. 855-882
96. Bevilacqua A, Neri A, De Martino P, Isaia R, Novellino A, Tramparulo FDA, Vitale S (2020) Radial interpolation of GPS and leveling data of ground deforma-tion in a resurgent caldera: application to Campi Flegrei (Italy). J Geodesy 94:24. https://doi.org/10.1007/s00190-020-01355-x
97. EGMS (2024) Dataset validated Ortho 2015-2021 (vector). European Ground Motion Service. doi: https://doi.org/10.2909/943e9cbb-f8ef-4378-966c-63eb761016a9
98. Lundgren P., Usai S., Sansosti E., Lanari R., Tesauro M., Fornaro G., Berardino P., 2001 Modeling surface deformation observed with synthetic aperture radar interferometry at Campi Flegrei caldera. Journal of Geophysical Research, 106, B9, 19.355-19.366.
99. Isaia R, Di Giuseppe MG, Natale J, Troiano A, Tramparulo FDA, Vitale S (2021) Volcano-tectonic setting of the Pisciarelli Fumarole Field, Campi Flegrei caldera, southern Italy: insights into fluid circulation patterns and hazard scenarios. Tectonics 40:e2020TC006227. https:// doi. org/ 10. 1029/ 2020TC006227
100. Petrosino, S., De Siena, L. Fluid migrations and volcanic earthquakes from depolarized ambient noise. Nat Commun 12, 6656 (2021). https://doi.org/10.1038/s41467-021-26954-w

 doi:10.20944/preprints202409.0809.v1

101. De Natale, G., Iannaccone, G., Martini, M. and Zollo, A. 1987. Seismic sources and attenuation properties at Campi Flegrei volcanic area. Pure Appl. Geoph., 125, 6, 883-917, 1987.
102. De Novellis, V.; Carlino, S.; Castaldo, R.; Tramelli, A.; De Luca, C.; Pino, N.A.; Pepe, S.; Convertito, V.; Zinno, I. The 21st August 2017 Ischia (Italy) earthquake source model inferred from seismological, GPS and DInSAR measurements. Geophys. Res. Lett. 2018, 45, 1–10.
103. De Natale, G., Zollo, A., Ferraro, A., Virieux, J., 1995. Accurate fault mechanism determinations for a 1984 earthquake swarm at Campi Flegrei caldera (Italy) during an unrest episode: implications for volcanological research. Journal of Geophysical Research, 100(B12).
104. Troise, C., De Natale, G., Pingue, F. and Zollo, 2003. A model for earthquake generation during unrest crises at Campi Flegrei and Rabaul calderas, Geophys. Res. Lett., 24, 13, 1575-1578, 1997.
105. Troise, C., De Natale, G., Pingue, F., Zollo, A., 1997. A model for earthquake generation during unrest episodes at Campi Flegrei and Rabaul calderas. Geophysical Research Letters, 24(13), pp. 1575–1578, 97GL01477
106. Mc Tigue, D.F. (1987) Elastic stress and deformation near a finite spherical magma body: resolution of the point source paradox. Jour. Geophys. Res., 92, B12, 12931-12940.